Clinical Neurophysiology 164 (2024) 119–129

Contents lists available at ScienceDirect

Clinical Neurophysiology

journal homepage: www.elsevier.com/locate/clinph

Redefined giant somatosensory evoked potentials: Evoked epileptic complexes of excitatory and inhibitory components

Haruka Ishibashi [a,b], Katsuya Kobayashi [a], Haruo Yamanaka [a], Maya Tojima [a], Kazuki Oi [a], Shuichiro Neshige [b], Takefumi Hitomi [c], Masao Matsuhashi [d], Hirofumi Maruyama [b], Ryosuke Takahashi [a], Akio Ikeda [d,*]

[a] Department of Neurology, Kyoto University Graduate School of Medicine, Japan
[b] Department of Clinical Neuroscience and Therapeutics, Hiroshima University Graduate School of Biomedical and Health Sciences, Japan
[c] Department of Clinical Laboratory Medicine, Kyoto University Graduate School of Medicine, Japan
[d] Department of Epilepsy, Movement Disorders and Physiology, Kyoto University Graduate School of Medicine, Japan

HIGHLIGHTS

- In the time–frequency analysis, P25 and N35 showed power increases of high-frequency activities in comparison to baseline activities, while P50 showed a power decrease.
- Short-latency of giant SEPs (P25 and N35) reflect evoked paroxysmal depolarization shifts.
- Middle latency of giant SEPs (P50) reflects the inhibitory component.

ARTICLE INFO

Article history:
Accepted 20 May 2024
Available online 27 May 2024

Keywords:
Somatosensory evoked potential
Giant SEP
Cortical myoclonus
Time–frequency analysis
Perampanel

ABSTRACT

Objective: Giant somatosensory evoked potentials (SEPs) are observed in patients with cortical myoclonus. Short-latency components (SLC), are regarded as evoked epileptic activities or paroxysmal depolarization shifts (PDSs). This study aimed to reveal the electrophysiological significance of the middle-latency component (MLC) P50 of the SEPs.
Methods: Twenty-two patients with cortical myoclonus having giant SEPs (patient group) and 15 healthy controls were included in this study. Waveform changes in SEPs before and after perampanel (PER) treatment were evaluated in the patient group. The wide range, time–frequency properties underlying the waveforms were compared between the groups.
Results: After PER treatment, SLC was prolonged and positively correlated with PER concentration, whereas MLC showed no correlation with PER concentration. Time–frequency analysis showed a power increase (156 Hz in all patients, 624 Hz in benign adult familial myoclonus epilepsy patients) underlying SLC and a power decrease (156 Hz, 624 Hz) underlying MLC in the patient group.
Conclusions: The high-frequency power increase in SLCs and decrease in MLCs clearly reflected PDS and subsequent hyperpolarization, respectively. This relationship was similar to that of interictal epileptiform discharges, suggesting that giant SEPs evoke epileptic complexes of excitatory and inhibitory components.
Significance: MLCs of giant SEPs reflected inhibitory components.

1. Introduction

Cortical myoclonus is an involuntary movement caused by cortical hyperexcitability and appears particularly in patients with progressive myoclonus epilepsy (PME), such as those with benign adult familial myoclonus epilepsy (BAFME), Unverricht-Lundborg disease (ULD), and Gaucher's disease (Ikeda et al., 1990;

* Corresponding author at: Department of Epilepsy, Movement Disorders and Physiology, Kyoto University Graduate School of Medicine, 54 Shogoin-Kawahara-cho, Sakyo-ku, Kyoto 606-8507, Japan.
E-mail address: akio@kuhp.kyoto-u.ac.jp (A. Ikeda).

https://doi.org/10.1016/j.clinph.2024.05.011
1388-2457/

Shibasaki et al., 1985). In patients with cortical (reflex) myoclonus, the following three electrophysiological findings can be specifically observed: giant somatosensory evoked potentials (SEPs), cortical reflex (C-reflex) or long-loop reflex, and a spike preceding spontaneous myoclonic jerks in jerk-locked back averaging (JLA). All of these are considered to represent cortical hyperexcitability or epileptic activity (Shibasaki et al., 1985; Ikeda et al., 1995; Shibasaki and Thompson, 2011). These studies have reported that the short-latency components (SLC, i.e., P25 and N35) of giant SEPs are equivalent to the excitatory components. More specifically, by comparing giant SEP and preceding spikes by JLA, it was suggested that the P25 of giant SEP was identical to the evoked epileptic spikes (Hallett et al., 1979; Shibasaki et al., 1985).

Perampanel (PER) is a selective non-competitive α-amino-e-h ydroxy-5-methyl-4-isoxazolepropionic acid (AMPA) receptor antagonist, which acts by inhibiting excitatory postsynaptic potential (EPSP) as well as paroxysmal depolarization shifts (PDSs) (Krauss et al., 2013). PDS is an abnormal giant EPSP that is thought to be associated with epileptogenicity (Matsumoto and Marsan, 1964). We recently examined and compared the clinical symptoms and giant SEP waveforms before and after the oral administration of PER. SLCs, that is, P25 and N35, showed temporal dispersion in terms of waveform morphology (prolonged latency and decreased amplitude) by the PER, and we concluded that the P25 and N35 components were electrophysiological representations of PDSs (Oi et al., 2019).

We recently reported that giant SEPs in BAFME patients were accompanied by high-frequency oscillations superimposed on the giant P25 (P25-HFOs) (Tojima et al., 2021a). HFOs in intracranial or scalp EEG are generally considered to reflect epileptogenicity (Bragin et al., 1999); thus, P25-HFOs may also reflect cortical hyperexcitability. As noted above, the SLCs of giant SEPs have been studied in relation to cortical hyperexcitability and epileptogenicity. (Hitomi et al., 2011; Kobayashi et al., 2011a; Kobayashi et al., 2014). However, there are few reports on the properties of the middle latency component (MLC) of giant SEPs (Ng and Jones, 2007; Shibasaki et al., 1985; Visani et al., 2013).

This study aimed to elucidate the electrophysiological significance of MLC of giant SEPs and whether both SLCs and MLCs are epileptic excitatory processes. Therefore, the MLC was evaluated and compared with the SLC from two perspectives: 1) changes in SEP findings before and after PER treatment and 2) high-frequency properties of the time–frequency analysis. We adopted a different method from that reported previously (Herrmann et al., 2014) in the time–frequency analysis.

2. Materials and methods

2.1. Subjects

This retrospective study included 21 patients with 1) cortical myoclonus and cortical tremor, and 2) unilateral or bilateral giant SEPs in response to median nerve stimulation. All patients were examined at Kyoto University Hospital between 2012 and 2020. The patients were diagnosed by board-certified neurologists based on family history, clinical symptoms, clinical course, neurophysiological examinations, neuroimaging tests, and genetic testing.

The clinical profiles of all the patients included in this study are shown in Table 1. The patient numbers included in each investigation are described in the footnotes of Table 1.

Among the 21 patients with cortical myoclonus or cortical tremor, 16 were diagnosed with BAFME, 3 with ULD, and 1 with Gaucher disease, and 1 with unclassified PME. Of the 16 patients with BAFME, 13 were diagnosed by genetic testing (Ishiura et al., 2018) and clinical diagnosis. The other three patients were clinically diagnosed with BAFME, two with definite and one with probable BAFME, based on clinical diagnostic criteria (Kobayashi et al., 2018). All three patients with ULD and one patient with Gaucher disease were genetically diagnosed. Patients with unclassified PME were diagnosed based on their clinical information.

We also used normal SEP data recorded in a previous report in 2011 (Hitomi et al., 2011). In a previous study, SEPs were recorded in 19 healthy controls (HCs). From those, the data in 15 control subjects (8 males and 7 females; mean age, 50.3 ± 18.4 years; range, 22–74 years) were adopted.

The Medical Research Ethics Committee of Kyoto University approved the study protocol (R0438/1625).

2.2. SEP recording and SLCs and MLCs

Scalp SEPs were recorded with either Viking (Nicolet, Biomedical, Madison, WI, USA) from 2012 to 2018 or Neuropack (Nihon Kohden Corp., Tokyo, Japan) from 2016 to 2020, using previously described recording procedures (Hitomi et al., 2011).

SEPs were recorded bilaterally in response to the median nerve stimulation of the wrist. Constant-current stimulation for a duration of 0.2 ms and a frequency of 1.1 Hz was repeated 50–250 times per side. The stimulus intensity was adjusted to 120 % of the motor threshold to produce a clear twitch in the thenar muscle. According to the international 10–20 system, electrodes were placed on C3′ and C4′ (2 cm posterior to C3 and C4) and referenced to an earlobe electrode placed ipsilateral to the electrical stimulation. The bandpass filter of the amplifier was set to 1–1500 Hz, and the sampling rate was set to 5–20 kHz. The analysis window after stimulation was 100 ms for the Viking and 200 ms for the Neuropack.

Although SEPs were recorded bilaterally in all patients, we adopted the SEP on the side with the larger amplitude in the P25 component. For patients who underwent SEPs examination multiple times, the side with the larger P25 amplitude at the first evaluation was used, and the same side was examined for all subsequent SEPs regardless of the amplitude value.

The nomenclature of the N20, P25, and N35 peaks was adopted from our previous study (Ikeda et al., 1995). Giant SEPs were defined when the P25 amplitude was > 6.3 μV or the N35 amplitude was > 9.8 μV (Ikeda et al., 1995), and as the inclusion criteria above indicate, all patients had giant SEPs at least on either side.

We defined the peak of the positive activity following N35 as "P50" accordingly as follows. This is because there have been no reports defining a positive component following N35 and because, in a preliminary evaluation of a few patients with giant SEPs, we confirmed that the positive peak following N35 appeared at approximately 50 ms.

The peak latency and amplitude were measured for each recognizable peak. When the giant SEP component showed bimodal peaks, the midpoint between the two peaks was used for analysis. We confirmed the reproducibility of SEP waveforms within the same recording. In each SEP recording, a half of the repeated trials were averaged alternately and the reproducibility was assessed in comparison of two waveforms from the same recording. Components with different shapes between the two waveforms and components with a difference in latency of more than 5 ms were excluded due to poor reproducibility.

2.3. Characteristics of giant SEP values

2.3.1. A comparison of SEP amplitude and latency

The flow of this study is shown in Fig. 1.

The amplitudes and latencies of each SEP component (N20, P25, N35, and P50) were compared between the patients (N = 18) and HCs (N = 15). In all 18 patients, SEP were assessed without PER treatment.

Table 1
Patient characteristics and clinical findings.

Pt no.	Disease (Age, gender)	Myoclonus score		Method 2.3.1 comparison to HC n = 17	Method 2.3.2 PER effects n = 9	Method 2.3.3 TFA n = 11	PER treatment		Concomitant drugs
		before PER	after PER				Final dose (mg/day) (mean ± SD) 2.6 ± 1.7	concentration per measurement (mg/dL)	
1	BAFME (64, F)	2	2	+	+	+	1	104	VPA, CZP
2	BAFME (49, F)	2	1	+	+	+	0.5	42	VPA, CZP
3	ULD (17, F)	3	3	+	+	+	3	78	VPA, PRM, CZP
4	BAFME (67, F)	2	1	+	+	+	3	NA	PHT
5	BAFME (62, M)	2	2	+	+	–	2	163	VPA, CZP
6	BAFME (46, F)	2	2	+	+	–	1	154, 203	VPA, CZP
7	BAFME (71, F)	3	3	+	+	–	1	197, 302	VPA, CZP
8	ULD (37, F)	3	2	+	+	–	4	690, 907, 906, 869, 830	VPA, LEV
9	GD (36, M)	2	1	+	+	–	7	344, 640	VPA, LEV
10	BAFME (71, F)	3	1	–	–	+	2	186	VPA, CZP, PER
11	BAFME (70, F)	1	0	–	–	+	4	372	VPA, CZP, PER
12	ULD (33, F)	3	3	–	–	+	2.5	539	VPA, TPM, CZP, PER
13	PME (30, F)	3	1	–	–	+	2.5	363	CZP, PER
14	BAFME (44, M)	2	–	+	–	+	–	–	CZP
15	BAFME (78, F)	3	–	+	–	+	–	–	VPA, CZP
16	BAFME (36, M)	2	–	+	–	+	–	–	VPA, LEV
17	BAFME (77, F)	3	–	+	–	–	–	–	LEV, VPA, PB, CZP
18	BAFME (30, F)	2	–	+	–	–	–	–	PB, CZP
19	BAFME (65, F)	2	–	+	–	–	–	–	CZP
20	BAFME (59, F)	1	–	+	–	–	–	–	VPA
21	BAFME (70, M)	1	–	+	–	–	–	–	LEV, VPA, CZP

Abbreviations: HC, healthy control; TFA, time–frequency analysis; PER, perampanel; SD, standard deviation; BAFME, benign adult familial myoclonus epilepsy; ULD, Unverricht-Lundborg disease; GD, Gaucher disease; PME progressive myoclonus epilepsy; M, male; F, female; NA, not available; VPA, sodium valproate; CZP, clonazepam; PRM, primidone; LEV, levetiracetam; PHT, phenytoin; TPM, topiramate; PB, phenobarbital.
Myoclonus score; Absence of myoclonus = 0, mild myoclonus without disturbance of daily activity = 1, some disturbance of daily activity = 2, clear disturbance of daily activity = 3 and causing incapacity = 4.
Patient characteristics and clinical findings.
In 17 patients (Pt 1–9, 14–21), SEPs before PER treatment were recorded, and they were compared with SEPs in healthy controls. (Method 2.3.1).
In 9 patients (Pt 1–9), SEPs before and after PER treatment were compared. (Method 2.3.2).
In 8 patients (Pt 1–3,5–9), changes in SEP latencies and amplitudes and the correlation of PER concentration were evaluated. The number of evaluations of the PER concentration in each patient was as follows; Pt 1–3,5: 1, Pt 6,7,9: 2; and Pt 8: 5. (See Methods 2.3.2). The daily PER dose was 2.6 mg on average (range: 0.5–7 mg) and the concentration for 8 patients (measured 15 times across patients) was 429 mg/dl (range: 42–906 mg/dl).
The single-sweep SEP data for the time–frequency analysis in relation to the SEP waveform were recorded in 11 patients (Pt 1–4, 10–16) (Method 2.3.3).

2.3.2. A comparison of giant SEP before and after PER treatment

Because the recording conditions and timing of PER treatment and SEP evaluation varied among patients, methods 2.3.1., 2.3.2., and 2.3.3., included patients who met the requirements for each method. Methods 2.3.1., included patients whose SEP was assessed before PER treatment, method 2.3.2., included patients whose SEP were assessed before and after PER treatment, and method 2.3.3 included patients with SEPs recorded in single-sweep trials.

We compared the SEP values of 9 patients before and after PER treatment. The methodological details for the comparison of SEP components before and after PER treatment are described in our previous report (Oi et al., 2019). In brief, to evaluate the influence of PER on SEP findings, we compared the amplitude and latency of giant SEP in nine patients (Pt 1–9). For patients who underwent multiple SEP evaluations after PER treatment, data from the first evaluation were used.

Importantly, we investigated the effect of PER on SEP values by correlating PER concentration with SEP amplitude/latency in eight patients (Pt 1–8) whose PER concentrations were evaluated. SEP and blood tests were performed within 6 months of PER initiation. Pt 9 was excluded because PER concentration was not assessed at the appropriate timing.

To specify the effect of PER concentration on each latency value of SEP, the interpeak latencies of P25-N35 and N35-P50, rather than the absolute latencies of P25, N35, and P50, were analyzed as important values before and after PER treatment. This is because the interpeak latencies of P25-N35 can selectively delineate the effect of the PER on the generator process of N35 by eliminating the effect on P25 in case of the absolute latency of P25. Similarly, the interpeak latency of N35-P50 could selectively delineate the effect of PER on P50, as opposed to the absolute latency of P50.

Absolute SEP amplitudes varied among patients; thus, we employed the amplitude attenuation rate to correlate with PER concentration. Similarly, the amplitude attenuation rate was calculated by dividing the difference before and after PER treatment with the amplitude before PER treatment.

2.3.3. Time–frequency analysis of giant SEPs

We analyzed time–frequency analysis of giant SEP data by using single sweep data set in 11 patients (Table 1, Pt 1–4, 10–16; 2 males, 49.9 ± 19.2 years old; 8 BAFME, 2 ULD, and 1 PME with unknown etiology).

Conventionally, a giant SEP waveform is obtained by averaging multiple trials time-locked to the stimulation; thus, the phase could vary in longer latency components. In the conventional method, in which time–frequency analysis is performed on a single waveform after averaging the trials, the activities (powers) of the MLC may be canceled out and underestimated. To overcome this problem, we applied time–frequency analysis to each single-sweep trial and averaged them, as was performed with studies of cognitive high-frequency activities, to obtain the activities corresponding to the SEP components (Herrmann et al., 2014).

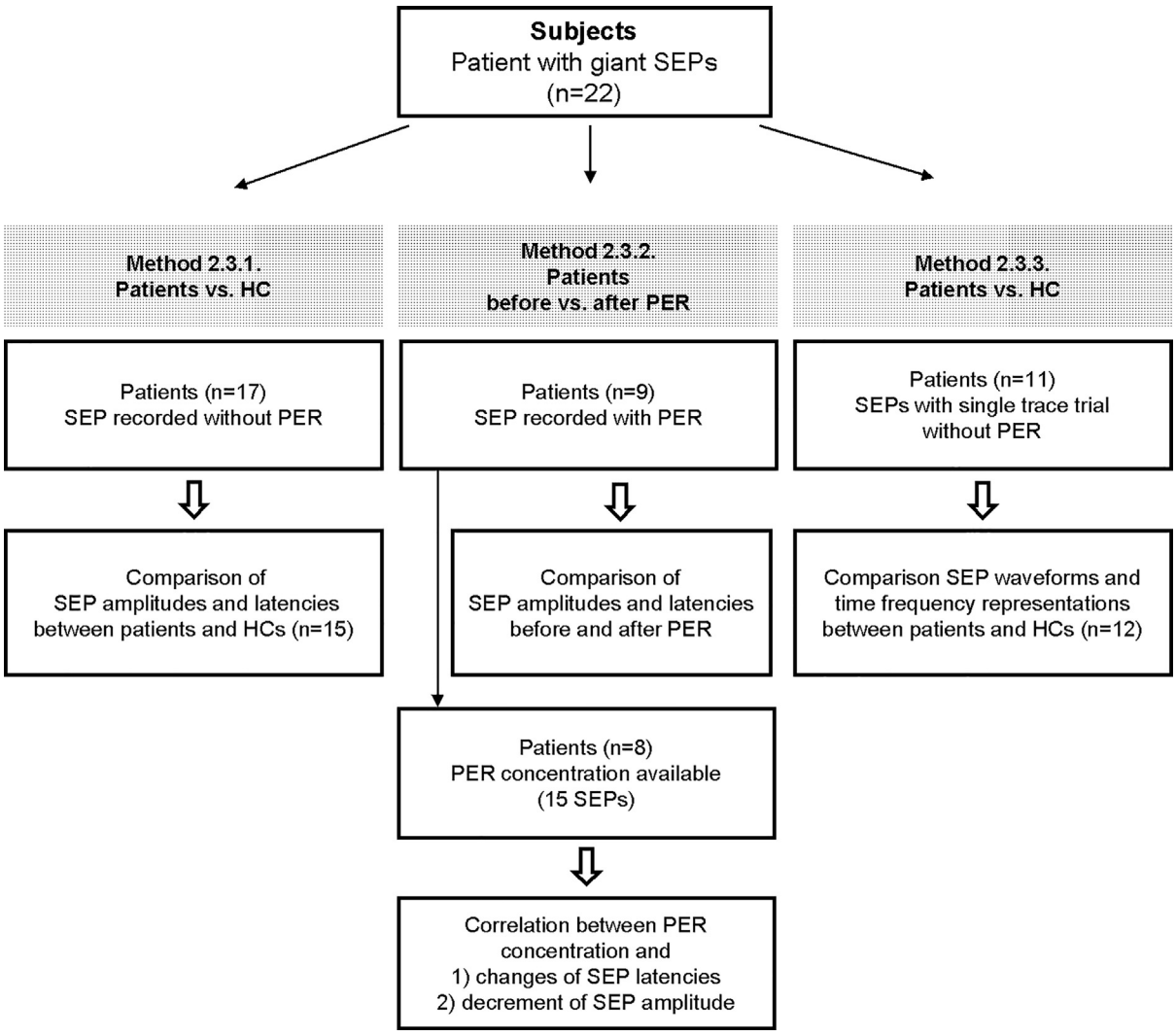

Fig. 1. Flowchart of the study. Twenty-two patients with giant SEPs were included. The timing of PER treatment and SEP evaluation varied between patients. Patients who met the conditions for each methodology were included in Methods 2.3.1, 2.3.2, and 2.3.3. Method 2.3.1 includes 17 patients and 15 HCs; method 2.3.2., 9 patients; and method 2.3.3., 11 patients and 12 HCs. SEP, somatosensory evoked potential; PER, perampanel; HC, healthy control.

To store single-sweep data, SEPs for time–frequency analysis were recorded using a Neuropack with a sampling rate of 10 kHz, and the analysis window after stimulation was set to 200 ms. Each single-sweep trial was analyzed as follows. A short-time Fourier transform (STFT) was used to obtain the power spectrum corresponding to each component of the SEP in the time domain. In this study, the fast Fourier transform (FFT) window was set to 6.4 ms (64 points), which corresponds to a frequency resolution of 156 Hz, and the FFT window was shifted every 1 ms. The power spectra of each trial were then averaged and expressed on a common logarithmic scale. The results of the time–frequency analysis were represented for every time bin (1 ms) and frequency band (156 Hz).

Only epochs with a false discovery rate < 0.01 were subsequently displayed to extract statistically significant power changes (increase or decrease) for the visual analysis. We considered that the power increase and decrease reflected the increment and suppression of the underlying neuronal activity, mainly as local field potentials. The latencies of N20, P25, N35, and P50 were measured in the averaged SEP waveform, and the associated corresponding power changes in the obtained time–frequency representation were demonstrated. Power changes were compared between 11 patients and 12 HCs for the specific frequency bands with outstanding power increases or decreases at the latencies of the targeted SEP components (i.e., N20, P25, N35, N35-P50, and P50 at 156 Hz and P25, N35-P50, and P50 at 624 Hz).

Table 2
Comparison in SEP components between patients with giant SEP and healthy controls.

	Patients n = 17	Healthy controls n = 15	P-value
Age, y (mean ± SD)	52.1 ± 18.5	50.3 ± 18.4	0.603
Male, n	5	9	
BAFME, n	14		
ULD, n	2		
Gaucher's disease, n	1		
Amplitude (μV)			
N20	3.5 ± 1.6	4.8 ± 2.1	0.025
P25	19.6 ± 10.2	7.0 ± 4.3	<0.001
N35	33.7 ± 19.8	3.5 ± 3.2	<0.001
P50	37.4 ± 17.2	5.8 ± 3.9	< 0.0001
Latency (ms)			
N20	17.9 ± 1.3	18.5 ± 1.4	0.24
P25	23.5 ± 1.1	24.8 ± 2.5	0.037
N35	33.5 ± 3.5	29.7 ± 1.5	<0.001
P50	57.2 ± 9.2*	41.0 ± 4.3	<0.0001

*One out of 18 was excluded due to poor reproducibility of P50 component.
Abbreviations: SD, standard deviation; BAFME, benign adult familial myoclonus epilepsy; ULD, Unverricht-Lundborg disease.

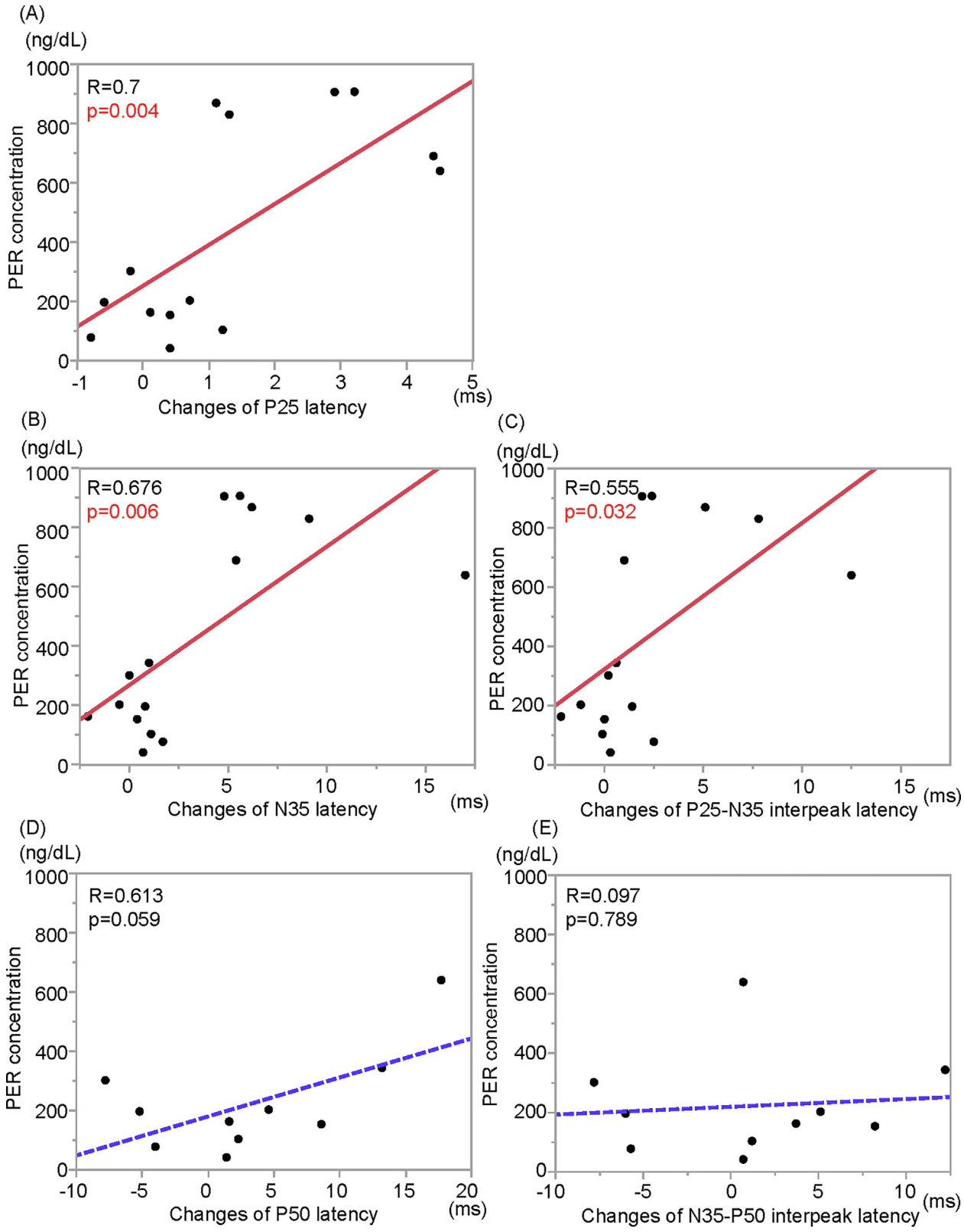

Fig. 2. Correlation between PER concentration and SEP latency. Data from 8 patients whose SEPs were examined before and after treatment were included. Changes in P25 (A), N35 (B), and P25-N35 interpeak latency (C) by PER were significantly correlated with PER blood concentration. No significant correlation was found between PER concentration and latency changes in the P50 (D) and N35-P50 interpeak latency (E). In four patients, the SEP recording and blood concentration test of PER were performed multiple times (Pt 1–3 and 9, once; Pt 6,7 and 9, twice; and Pt 8, 5 times), and all were included in the investigation. Note that the P50 components of Pt 8 were excluded due to poor reproducibility. PER, perampanel; SEP, somatosensory evoked potentialt.

2.4. Statistical analysis

Signal processing of all SEP waveforms was performed using in-house MATLAB scripts applicable for offline analyses (R2021b; MathWorks Ltd., MA). Clinical profiles, amplitude, and latency of SEP components between patients and HCs, and the power changes corresponding to SEP components between patients and HCs were evaluated using a *t*-test. Changes in each component before and after PER treatment were evaluated using paired t-tests. Correlations between SEP components and PER concentrations were analyzed using the Pearson correlation coefficient. All Statistical evaluations were performed using the JMP software (Pro version 16.1.0; SAS Institute, Cary, NC, USA). Statistical significance was set at $p < 0.05$.

3. Results

3.1. Characteristics of giant SEP values

First, the reproducibility of all waveforms was checked. The P50 components in the 5 recordings of Pt 8 were excluded from all analysis due to poor reproducibility.

The mean age of the 17 patients included in method 2.3.1 (52.1 ± 18.5, 5 males) was like that of 15 HCs ($p = 0.603$, Table 2). All patients had been treated with anti-seizure or anti-myoclonus medications, including PER: PER in 9 patients, valproic acid in 14 patients, clonazepam in 12 patients, levetiracetam in 5 patients, phenobarbital in 2 patients, and phenytoin and primidone in 1 patient (Table 1).

The giant SEPs of patients had a larger amplitude than the SEPs of HCs for P25, N35, and P50 (all $p < 0.001$). The latency of giant SEPs in the patient group was significantly longer than that in the HC group for N35 ($p = 0.0002$) and P50 ($p < 0.0001$), but not for P25 ($p = 0.037$) (Table 2). The amplitudes and latencies of N20 did not differ between the patients and HCs.

3.2. Comparison of giant SEP before and after PER treatment

The average interval between SEP recording before and after PER treatment in the nine patients was 23 months (range: 6–54 months). The shortest interval between PER treatment and subsequent SEP recording was at least one month, which was sufficient to reach steady-state blood concentrations of PER.

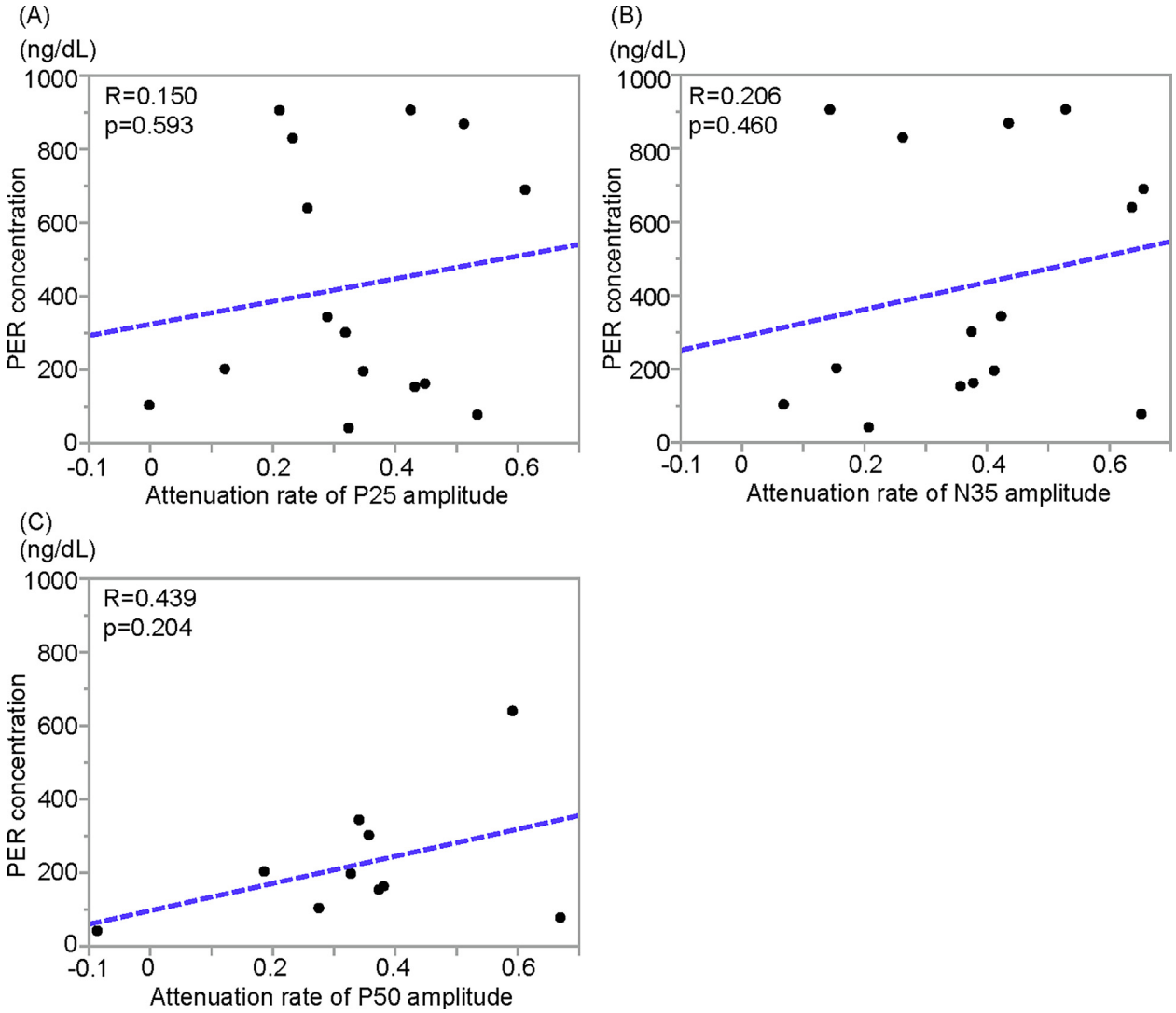

Fig. 3. Correlation between PER concentration and attenuation rate of SEP amplitudes. Data from 8 patients whose SEPs were examined before and after PER treatment were included. A correlation was observed between PER concentration and the attenuation rate of amplitude after PER treatment. Changes in amplitude did not significantly correlate with PER concentrations in any of the components (A, B, and C). PER, perampanel; SEP, somatosensory evoked potential.

The amplitudes of all giant SEP components decreased significantly after PER treatment (P25, p = 0.01; N35, p = 0.014; P50, p = 0.02), whereas there was no difference in latencies (P25, p = 0.19; N35, p = 0.12; P50, p = 0.32) (Supplementary Table 1). The N20 amplitude and latency showed no difference before and after PER administration (amplitude, p = 0.78; latency, p = 0.351).

Correlations between PER concentration and SEP amplitude, and latency were evaluated in eight patients (Pt 1–8). The daily PER dose was 2.6 mg on average (range: 0.5–7 mg) and the concentration for 8 patients (measured 15 times across patients) was 429 mg/dl (range: 42–906 mg/dl).

There was a significant positive correlation of PER concentration with P25 latency (R = 0.7, p = 0.004) (Fig. 2A) and N35 latency (R = 0.676, p = 0.006), and with P25-N35 interpeak latency (R = 0.555, p = 0.032) (Fig. 2B, C), whereas no correlation was seen with interpeak latency of P50 (R = 0.613, p = 0.059) or N35-P50 (R = 0.097, p = 0.789) (Fig. 2D, E). The PER concentration did not correlate with the attenuation of amplitude at P25 (R = 0.150, p = 0.593), N35 (R = 0.206, p = 0.460), or P50 (R = 0.439, p = 0.204) (Fig. 3A, B, C).

3.3. Time–frequency analysis of giant SEPs

As a single-subject data display, Fig. 4 shows the time–frequency representation associated with giant SEPs in a patient with BAFME and HC. A power increase was observed in the frequency band below 400 Hz, which is consistent with the peak latencies of P25 and N35, and to a much lesser degree, at N20. In addition, a power increase at P25 was observed in the frequency band above 400 Hz in seven patients with BAFME. In contrast, a wide-band but rather scattered power decrease was observed from the N35 peak to the P50 peak (Fig. 4A). In comparison, none of these findings were observed in the HC.

In the group comparison, evaluation of the time–frequency representation associated with giant SEPs in 11 patients showed power increases corresponding to N20, P25, and N35 in all patients. A power increase consistent with P25 at frequencies above 400 Hz was observed in seven patients with BAFME. None of the patients showed a power increase consistent with the peak latency of the P50. In seven patients, a broadband power decrease was observed between the N35 and P50 peaks.

Logarithmic power changes with reference to baseline activities were compared between the patient and HC groups (Fig. 5, Supplementary Table 2). In the patient group, a significant power increase was observed in the frequency band at approximately 156 Hz at the peak latencies of P25 and N35 (P25; p < 0.001, N35; p = 0.0003), and the power increased at approximately 612 Hz at P25 (p = 0.0009). In addition, a significant decrease in power was observed in the patient group between the N35 and P50 peaks in both frequency bands (156 Hz, p < 0.0001; 624 Hz, p < 0.0001).

4. Discussion

This study delineates, for the first time, a clear difference between the SLCs and MLCs of giant SEPs (P25 and N35 vs. P50) from the following 2 perspectives, namely responsiveness to PER and time–frequency analysis. (1) PER did not affect P50 latency or N35-P50 inter-peak latency, whereas PER prolonged P25 and N35 latencies, and (2) a power decrease was observed at the MLC, that is, between the segment after the N35 peak toward P50, whereas a power increase was observed at the SLCs, that are P25 and N35. We consider that the giant P25 and N35 components correspond to evoked epileptic activity and that P50 reflects subsequent suppression following excitation.

Previous studies have evaluated only giant SEPs up to N35 (Alegre et al., 2006; Shibasaki et al., 1985). Giant SEP in the previous report were presented until a latency of 200 ms, and a positive

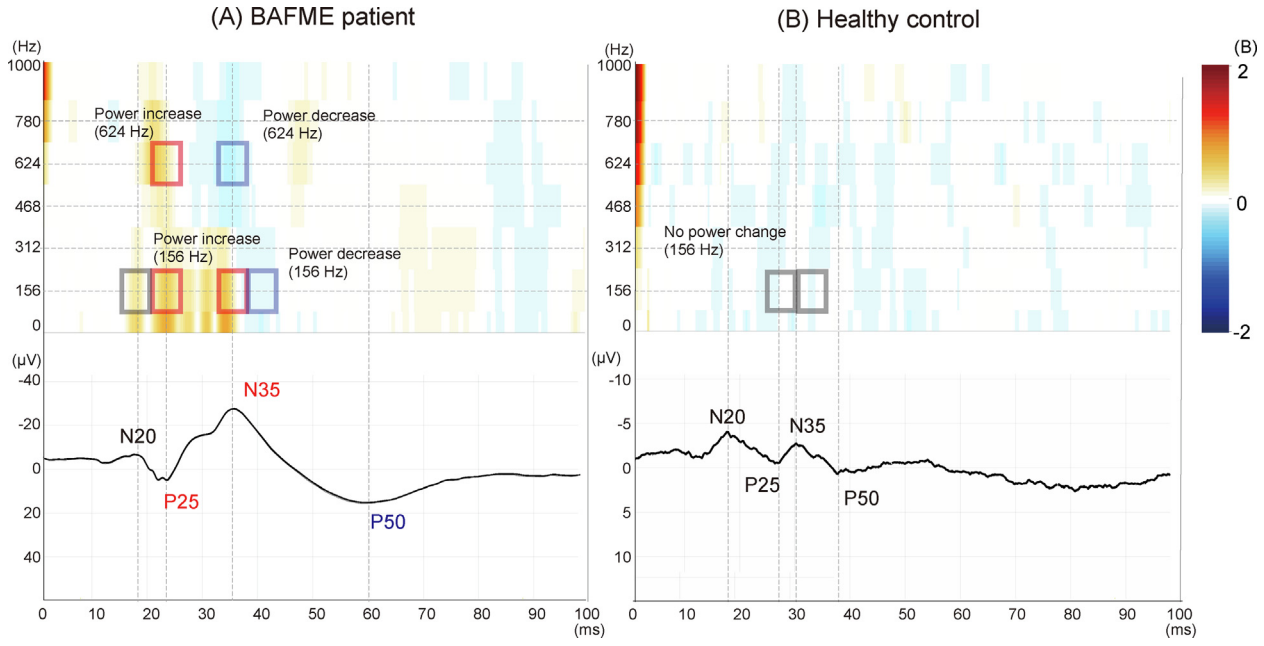

Fig. 4. Time–frequency representation and SEP waveform in a representative patient with BAFME and healthy control. (A): SEP waveform and its time–frequency representation in a patient with BAFME (Pt 2, 49-years old female). (B): SEP waveform and its time–frequency representation in a healthy 28-year-old male. (A) shows a power increase below 400 Hz, consistent with the peak latency of the P25 and N35 components (red rectangles) and no power change in the N20 component (gray rectangles). A power increase at P25 is observed in the frequency band above 400 Hz (red rectangle), particularly in patients with BAFME. A wideband power decrease was observed from the N35 peak to the P50 peak (blue rectangle). (B) shows no power change below 400 Hz, which is consistent with the P25 and N35 components (gray rectangle) and no other power changes. SEP, somatosensory evoked potential; BAFME, benign adult familial myoclonic epilepsy. (For interpretation of the references to colour in this figure legend, the reader is referred to the web version of this article.)

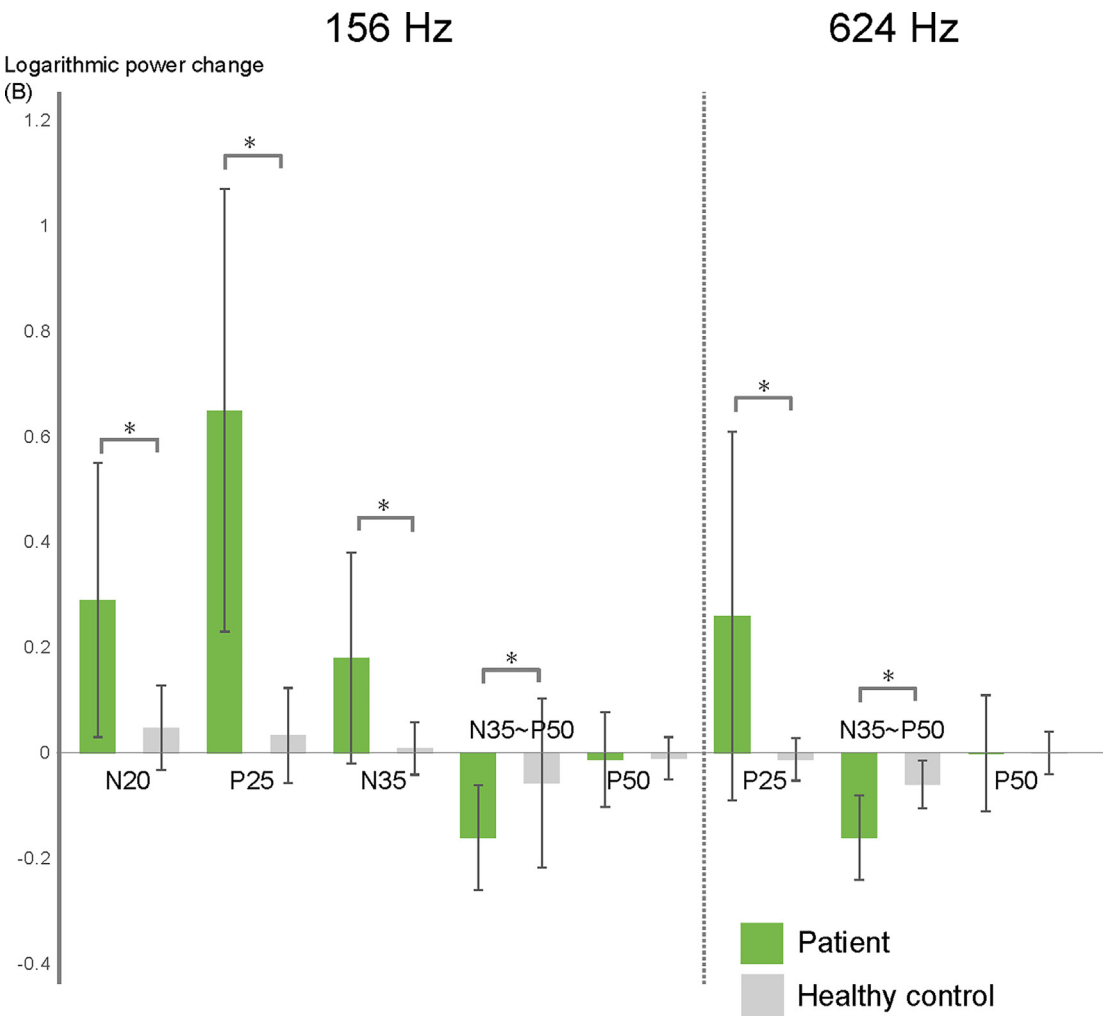

Fig. 5. Comparison of power changes corresponding to SLCs and MLCs of SEPs between patients and HCs Logarithmic power changes in reference to baseline activities were compared between patients and healthy controls. * indicates $p < 0.05$. In the patient group, a significant power increase was observed in the frequency band around 156 Hz at the peak latencies of P25 and N35 (P25, $p < 0.001$; N35, $p = 0.0003$), and a significant power increase around 612 Hz at P25 ($p = 0.0009$) in the patient group. A significant decrease in power was observed between N35 and P50 in both frequency bands (156 Hz, $p < 0.0001$; 624 Hz, $p < 0.0001$). SLC, short latency component; MLC, middle latency component; SEP, somatosensory evoked potential; HC, healthy control.

component could be identified around 50–60 ms following N35 (Shibasaki et al., 1985). This positive component, although not clearly described, is most likely the P50 in the current study. (Shibasaki et al., 1985; Shibasaki et al., 1977). Also, Visami et al. evaluated the SEP recovery function (SEP-R) in ULD patients with giant SEP and argued that the response to the second stimulus was influenced by the suppression component of the middle latency component of giant SEP. Although they defined the positive component around the latency of 150 ms as 'middle latency', which is different from ours, a period of "refractoriness" following extreme depolarization as indicated by giant SEPs might be one of the underlying factors of suppression in the middle latency components.

Functional decomposition between SLCs and MLCs may help us understand the pathophysiology of cortical myoclonus and may help us evaluate treatment efficacy and predit clinical course of patients.

4.1. Difference in significance of SLCs and MLCs between giant SEPs and normal SEPs

Based on previous reports, the SLCs of giant SEPs are recognized as equivalent to the evoked PDS to the afferent input. In normal SEPs, N20-P30 is recorded as a potential generated from Brodmann area 3b, and the N20 origin is an EPSP (Allison et al., 1989).

In giant SEPs, the P25 and N35 components are abnormally enlarged, while N20 is not, suggesting that N20 can be an ordinary EPSP like a normal SEP.

Similar to the spontaneous epileptic spikes such as PDS, the generator mechanism of the SLC of giant SEPs is regarded as evoked PDS to afferent input, as shown by the JLA method and SEP/C-reflex. The finding that PER, a selective AMPA receptor antagonist, causes P25 prolongation is most likely interpreted as a temporal dispersion of the P25 component (Oi et al., 2019), and finally it also supports that P25 reflects PDS.

There have been only a few reports on the MLCs of normal SEPs. Allison et al. reported that P20-N30-P45-N80-P180, and N20-P30-N45-P80-N180 were recorded in the frontal and parietal regions, respectively (Allison et al., 1989). The middle-latency, normal SEP components are considered to be the activation of associative cortical areas via cortico-cortical connections or cortical responses to inputs from the thalamus.

In this study, we compared the amplitudes and latencies of the SLCs and MLCs of giant SEPs with those of normal SEPs. The amplitudes of P25, N35, and P50 were markedly increased compared with those in healthy subjects. In contrast, the latencies of N35

and P50 in patients were prolonged compared with those in healthy subjects, while the latency of N20 did not change (P25 may be marginally prolonged). The prolonged latency of the components following N20 in patients is consistent with previous reports (Shibasaki et al., 1985). The fact that the latencies of P50 differed between cortical myoclonus patients and HCs could be explained by that the components following P25 and N35 in giant SEPs represent pathological activities of abnormal cortical origin. In general, interictal epileptiform discharges consist of spikes reflecting PDS and following post-spike slow, which is considered an inhibitory component. The relationship between the short-latency P25/N35 and middle-latency P50 in giant SEPs may be equivalent to that of interictal epileptiform discharges and subsequent post-spike slow components, respectively.

4.2. Significance of MLCs of giant SEPs

First, giant P25 and N35 showed prolonged latencies that correlated with the blood concentration of PER, which was interpreted as the temporal dispersion of potentials caused by PER (Oi et al., 2019). In contrast, P50 behaved differently from P25/N35. The amplitude of P50 decreased, whereas there was no correlation between prolonged latencies and the blood concentration of PER. Considering that the latencies of P50 were shortened after PER treatment up to 7.8 ms in three patients, P50 may not necessarily be the component affected by PER that desynchronizes cortical activities. This result is consistent with the hypothesis that middle-latency SEP may be an inhibitory component reflecting the suppression of neuronal activity following PDS (Fig. 6).

Second, the time–frequency representation of giant SEPs can help clarify the characteristics of each component of giant SEP SLCs and MLCs, such as P50, as is done for epileptic spikes (Jacobs et al., 2011; Kobayashi et al., 2011b).

In this study, we revealed a power increase at the P25 and N35 peaks, and a power decrease consistently around the N35-P50 segment (from the descending part of N35 toward the P50 peak) in seven of 11 patients. It is noteworthy that, regarding the interictal epileptiform discharge recorded in patients with epilepsy, power increases at the spike component and power decreases during subsequent slow waves have been observed, especially in intracranial electroencephalography recordings (Jacobs et al., 2011; Kobayashi et al., 2011b). The power decrease following the spike components is consistent with the suppression of neuronal excitation, reflecting hyperpolarization (Urrestarazu et al., 2006). Hence, as observed in the giant SEP waveforms, the SEP component after N35 (N35-P50) showing a power decrease may correspond exactly to post-spike suppression in interictal epileptiform discharges following PDS. Although a power decrease was observed in seven of 11 patients, factors related to this could not be examined due to the limited number of patients, and evaluation with a larger number of subjects may be needed to further clarify this point.

In addition, a power increase in the high-frequency band (>400 Hz), consistent with P25, was observed in seven patients, all of whom were BAFME patients. This activity was equivalent to that of P25-HFO in BAFME, as recently reported by our group

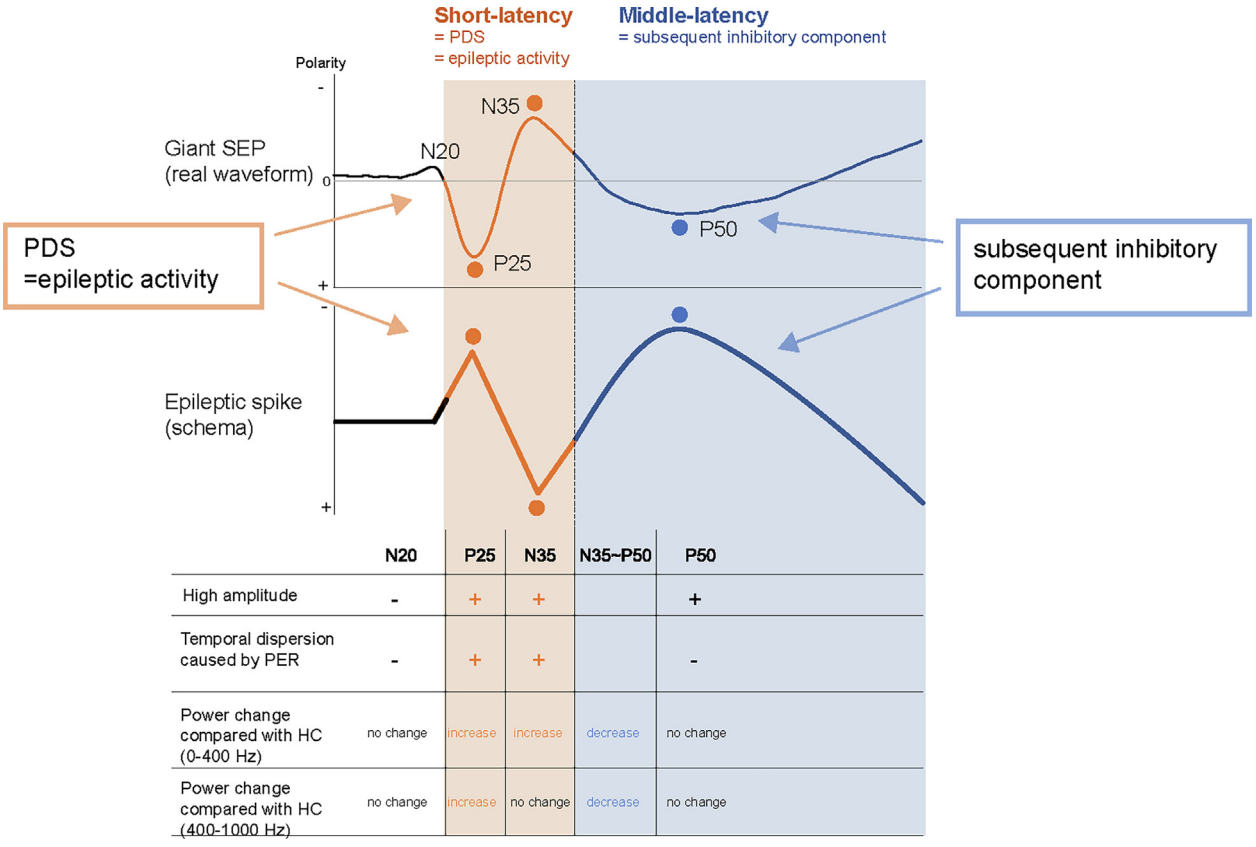

	N20	P25	N35	N35~P50	P50
High amplitude	-	+	+		+
Temporal dispersion caused by PER	-	+	+		-
Power change compared with HC (0-400 Hz)	no change	increase	increase	decrease	no change
Power change compared with HC (400-1000 Hz)	no change	increase	no change	decrease	no change

Fig. 6. The hypothesis of the electrophysiological mechanism of giant SEP components. The relationship between SLCs (P25/N35) and MLCs (P50) in giant SEPs was similar in morphology to the waveform observed in interictal epileptiform discharges. The reason for the reversed polarity of epileptic spikes and giant SEPs is that giant SEPs are evoked potentials, and the potential generated in the deep layer of the cerebral cortex is reversed at the surface, whereas epileptic spikes are spontaneous discharges with superficial negativity. SEP, somatosensory evoked potential; PDS, paroxysmal depolarization shifts; PER, perampanel; HC, healthy control; SLC, short latency component; MLC, middle latency component.

(Tojima et al., 2021a). It is a highly sensitive and specific biomarker for the diagnosis of BAFME and is thought to reflect the pathological hyperexcitation of the primary sensorimotor cortex and the normal cerebellar efferent input system.

4.3. Limitation

First, this was a retrospective study with a limited follow-up period. Several factors may have influenced these results. 1) SEP findings before and after PER treatment may be partially affected by other medications and aging (Rothwell et al., 1984; Hitomi et al., 2011). However, PER is the only drug reported to cause temporal dispersion in SEP waveforms (Oi et al., 2019). We recently published more than 10 years of follow-up of giant SEPs investigating the effects of various ASMs and found that only PER could produce dramatically prolonged latency (Tojima et al., 2021b). 2) P50 component data of Pt 8 were excluded due to poor reproducibility. This made the evaluation of correlations between PER concentrations and MLC at lower concentrations compared to SLC, and might have affected the results to some extent. 3) All patients had PME syndrome; however, each diagnosis varied, including BAFME, ULD, Gaucher disease, and unknown cortical myoclonus. Further evaluation is needed to clarify the disease-specific characteristics of MLC in each disease.

5. Conclusion

In this study, we functionally redefined the SLC and MLCs of giant SEP in terms of 1) waveform characteristics, 2) mode of response to PER, and 3) power changes in the time–frequency analysis associated with giant SEPs. The SLCs (P25 and N35) and MLC (P50) behaved differently; SLCs may be considered as PDSs, and MLC as having most likely compatible inhibitory activities. The functional structures of giant SEPs and their associates are morphologically similar to those observed in interictal epileptiform discharges, suggesting that giant SEPs may be a phenomenon similar to stimulus-induced PDSs.

Conflict of interest statement

Akio Ikeda and Masao Matsuhashi are current members of the Department of Epilepsy, Movement Disorders and Physiology (Kyoto University Graduate School of Medicine). This department is the Industry-Academic Collaboration Courses, supported by Eisai Co., Ltd., NIHON KOHDEN CORPORATION, Otsuka Pharmaceutical Co., and UCB Japan Co., Ltd.

None of the authors has any conflicts of interest to disclose in relation to this study.

CRediT authorship contribution statement

Haruka Ishibashi: Data curation, Formal analysis, Visualization, Writing – original draft, Writing – review & editing. **Katsuya Kobayashi:** Conceptualization, Formal analysis, Funding acquisition, Methodology, Visualization, Supervision, Writing – review & editing. **Haruo Yamanaka:** Formal analysis, Writing – review & editing. **Maya Tojima:** Data curation, Formal analysis, Visualization, Writing – review & editing. **Kazuki Oi:** Writing – review & editing. **Shuichiro Neshige:** Writing – review & editing. **Takefumi Hitomi:** Data curation, Funding acquisition, Supervision, Writing – review & editing. **Masao Matsuhashi:** Methodology, Software, Writing – review & editing. **Hirofumi Maruyama:** Writing – review & editing. **Ryosuke Takahashi:** Writing – review & editing. **Akio Ikeda:** Conceptualization, Funding acquisition, Resources, Supervision, Writing – review & editing.

Acknowledgement

This study was supported by Health and Labor Sciences Research Grants on Rare and Intractable Disease from the Ministry of Health, Labour and Welfare, Japan (20FC1039), a Grant-in-Aid for Scientific Research (B) KAKENHI Grant Number 19H03574, a Grant-in-Aid for Scientific Research (C) KAKENHI Grant Number 20 K07902, a Grant-in-Aid for Challenging Exploratory Research KAKENHI Grant Number 20 K21573, and a Grant-in-Aid for Early-Career Scientists KAKENHI Grant Number 22 K15729 from the Ministry of Education, Culture, Sports, Science and Technology (MEXT), Japan.

Appendix A. Supplementary material

Supplementary data to this article can be found online at https://doi.org/10.1016/j.clinph.2024.05.011.

References

Alegre M, Urriza J, Valencia M, Muruzábal J, Iriarte J, Artieda J. High-frequency oscillations in the somatosensory evoked potentials of patients with cortical myoclonus: pathophysiologic implications. J Clin Neurophysiol 2006;23(3):265–72.
Allison T, McCarthy G, Wood CC, Williamson PD, Spencer DD. Human cortical potentials evoked by stimulation of the median nerve. II. Cytoarchitectonic areas generating long-latency activity. J Neurophysiol 1989;62(3):711–22.
Bragin A, Engel Jr J, Wilson CL, Fried I, Buzsáki G. High-frequency oscillations in human brain. Hippocampus 1999;9(2):137–42.
Hallett M, Chadwick D, Marsden CD. Cortical reflex myoclonus. Neurology 1979;29(8):1107–25.
Herrmann CS, Rach S, Vosskuhl J, Strüber D. Time-frequency analysis of event-related potentials: a brief tutorial. Brain Topogr 2014;27(4):438–50.
Hitomi T, Ikeda A, Kondo T, Imamura H, Inouchi M, Matsumoto R, et al. Increased cortical hyperexcitability and exaggerated myoclonus with aging in benign adult familial myoclonus epilepsy. Mov Disord 2011;26(8):1509–14.
Ikeda A, Kakigi R, Funai N, Neshige R, Kuroda Y, Shibasaki H. Cortical tremor: a variant of cortical reflex myoclonus. Neurology 1990;40(10):1561–5.
Ikeda A, Shibasaki H, Nagamine T, Xu X, Terada K, Mima T, et al. Peri-rolandic and fronto-parietal components of scalp-recorded giant SEPs in cortical myoclonus. Electroencephalogr Clin Neurophysiol 1995;96(4):300–9.
Ishiura H, Doi K, Mitsui J, Yoshimura J, Matsukawa MK, Fujiyama A, et al. Expansions of intronic TTTCA and TTTTA repeats in benign adult familial myoclonic epilepsy. Nature Gene 2018;50(4):581–90.
Jacobs J, Kobayashi K, Gotman J. High-frequency changes during interictal spikes detected by time-frequency analysis. Clin Neurophysiol 2011;122(1):32–42.
Kobayashi K, Hitomi T, Matsumoto R, Kondo T, Kawamata J, Matsuhashi M, et al. Long-term follow-up of cortical hyperexcitability in Japanese Unverricht-Lundborg disease. Seizure 2014;23(9):746–50.
Kobayashi K, Hitomi T, Matsumoto R, Watanabe M, Takahashi R, Ikeda A. Nationwide survey in Japan endorsed diagnostic criteria of benign adult familial myoclonus epilepsy. Seizure 2018;61:14–22.
Kobayashi K, Matsumoto R, Kondo T, Kawamata J, Hitomi T, Inouchi M, et al. Decreased cortical excitability in Unverricht-Lundborg disease in the long-term follow-up: a consecutive SEP study. Clin Neurophysiol 2011a;122(8):1617–21.
Kobayashi K, Yoshinaga H, Toda Y, Inoue T, Oka M, Ohtsuka Y. High-frequency oscillations in idiopathic partial epilepsy of childhood. Epilepsia 2011b;52(10):1812–9.
Krauss GL, Perucca E, Ben-Menachem E, Kwan P, Shih JJ, Squillacote D, et al. Perampanel, a selective, noncompetitive α-amino-3-hydroxy-5-methyl-4-isoxazolepropionic acid receptor antagonist, as adjunctive therapy for refractory partial-onset seizures: interim results from phase III, extension study 307. Epilepsia 2013;54(1):126–34.
Matsumoto H, Marsan CA. Cortical cellular phenomena in experimental epilepsy: interictal manifestations. Exp Neurol 1964;9:286–304.
Ng K, Jones S. The, "enhanced N35" somatosensory evoked potential: its associations and potential utility in the clinical evaluation of dystonia and myoclonus. J Neurol 2007;254(1):46–52.
Oi K, Neshige S, Hitomi T, Kobayashi K, Tojima M, Matsuhashi M, et al. Low-dose perampanel improves refractory cortical myoclonus by the dispersed and suppressed paroxysmal depolarization shifts in the sensorimotor cortex. Clin Neurophysiol 2019;130(10):1804–12.
Rothwell JC, Obeso JA, Marsden CD. On the significance of giant somatosensory evoked potentials in cortical myoclonus. J Neurol Neurosurg Psychiatry 1984;47(1):33–42.

Shibasaki H, Thompson PD. Milestones in myoclonus. Mov Disord 2011;26 (6):1142–8.
Shibasaki H, Yamashita Y, Neshige R, Tobimatsu S, Fukui R. Pathogenesis of giant somatosensory evoked potentials in progressive myoclonic epilepsy. Brain 1985;108(Pt 1):225–40.
Shibasaki H, Yamashita Y, Tsuji S. Somatosensory evoked potentials. Diagnostic criteria and abnormalities in cerebral lesions. J Neurol Sci 1977;34(3):427–39.
Tojima M, Hitomi T, Matsuhashi M, Neshige S, Usami K, Oi K, et al. A biomarker for benign adult familial myoclonus epilepsy: high-frequency activities in giant somatosensory evoked potentials. Mov Disord 2021.
Tojima M, Takahashi R, Neshige S, Hitomi T, Matsuhashi M, Ikeda A. Marked response to perampanel: a decade-long course of giant somatosensory evoked potentials in Unverricht-Lundborg disease. Clin Neurophysiol 2021b;132 (10):2329–31.
Urrestarazu E, Jirsch JD, LeVan P, Hall J, Avoli M, Dubeau F, et al. High-frequency intracerebral EEG activity (100–500 Hz) following interictal spikes. Epilepsia 2006;47(9):1465–76.
Visani E, Canafoglia L, Rossi Sebastiano D, Agazzi P, Panzica F, Scaioli V, et al. Giant SEPs and SEP-recovery function in Unverricht-Lundborg disease. Clin Neurophysiol 2013;124(5):1013–8.